Assessment of the 3D geometrical effects on the DEMO divertor pumping efficiency

S. Varoutis*, Yu. Igitkhanov, Chr. Day

Karlsruhe Institute of Technology (KIT), Institute of Technical Physics, Vacuum Department, Karlsruhe, Germany

ABSTRACT

In the present work, a parametric analysis by using the DIVGAS code is performed in order to highlight the influence of the inter-cassette gaps and the existence of the dome on the overall pumping efficiency of the DEMO divertor. For this fundamental study, a 3D divertor configuration is chosen, in which deuterium neutral particles are assumed to penetrate the private flux region. The chosen incoming boundary conditions correspond to high-collisionality divertor operational conditions. It has been found that in the case for a divertor without a dome the particle losses through the separatrix are dominating and consequently the effect of 3D leakages on the pumping efficiency is small. For the reference case of 20 mm gap width with the dome and low capture coefficients, the pumping efficiency is 9 times higher than for the case without the dome. In general, the existence of dome results in the elimination of the outflux of neutrals towards the x-point and forces the neutrals to move towards the sub-divertor vicinity, finally achieving a neutral compression. It is shown that the dome provides a first order variation in pumping efficiency in comparison to the case of the divertor without the dome, while the gap leakages provide a second order variation, which seems to be more important when the dome is present.

1. Introduction

The DEMO divertor system comprises 54 individual cassettes. The cassettes are not perfectly sealed but have, for reasons of mechanical tolerances, gaps between each other. As a consequence, unintended particle fluxes will occur both in poloidal and toroidal directions and between the divertor cassettes. This issue has been already investigated for the case of Alcator C-Mod [1], in which the influence of the gaps in the poloidal and toroidal direction is significant and only if their existence is assumed, the corresponding numerical and experimental results may coincide. Furthermore, the same study has been performed for the case of ITER [2], where the simulations indicate that the parasitic flows caused by these gaps can be comparable to the pumping throughput. Similar conclusions were drawn in [3] where it has been found that a very strong back streaming of gas into the plasma occurs, mainly due to the flows through the inter-cassettes gaps. Furthermore, a recent study has been performed for the case of a 3D DEMO divertor [4] without a dome in which the assumed divertor plasma conditions correspond to low divertor pressure levels (i.e. low divertor collisionality). This work has for the first time introduced the aspect of the pumping efficiency, defined as the ratio of the pumped over the net incoming neutral particle flux, considering the inter-cassettes gaps. There, the analysis has shown that for small gaps the pumping efficiency is almost independent of the gap width, while for large values of the gap width the pumping efficiency may be reduced by 20%. Furthermore, as there is no dome, almost 80% of the incoming to private flux region (PFR) neutral particles were found to move towards the x-point, independent of the gap width.

The present work is a continuation of the study presented in [4], in which the main divertor 3D geometry was kept the same but additionally the dome structure has been added as well as higher divertor pressure levels in PFR (i.e. high divertor collisionality), more relevant to DEMO operational conditions, have been assumed. Regarding the presence of the dome, it is noted that its primary function is to achieve a high compression of neutrals in the PFR in order to increase the pumping efficiency. Additionally, the dome may reduce the neutral outflux towards the plasma core through the x-point and shield the pumping port against neutrons.

The present analysis will allow defining the design space and the impact of the dome and the inter-cassettes gaps on the overall pumping efficiency of the DEMO divertor, which is still under an ongoing conceptual design phase. The ultimate goal is to define an optimum divertor design in terms of its pumping efficiency, using as the main driver the particle transport physics.
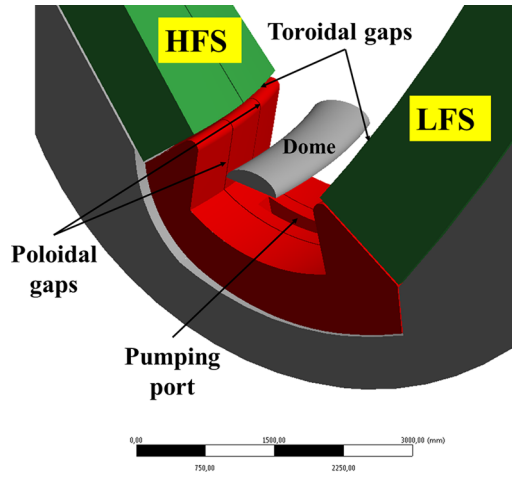
Fig. 1. Three dimensional DEMO 2015 divertor configuration including three divertor cassettes, the dome, the first wall and the surrounding vacuum vessel.

2. Divertor geometry

The current model of a 20° degree DEMO divertor segment is shown in Fig. 1. The presented divertor configuration is based on the 2015 EU DEMO baseline design [5], which includes in total 54 divertor cassettes and has a major radius equal to $R = 9.1$ m. Five different geometrical configurations have been studied in which the width d of the poloidal and toroidal gaps varies between 0 and 40 mm. The inter-cassette gap width equal to 20 mm is assumed here as a reference case. In Fig. 2a, the 3D DEMO divertor configuration, which corresponds to a 20° degree sector and includes the dome and the toroidal and poloidal gaps, is shown. For representation purposes, the plane KK´ is additionally introduced.

In Fig. 2b, a 2D cut along the KK´ plane of the applied 3D model is depicted. In this specific design, the particles, which enter the pumping port and reach its outlet, have the possibility to flow in the toroidal or poloidal direction (not shown here) in the volume between the divertor cassette and the vacuum vessel. The adsorbing surface D named as pumping slot in this case is located further below the pumping port outlet and a given capture coefficient ξ (i.e. the probability of a particle to be pumped from there) is appointed. Consequently, ξ takes values between $0 \leq \xi \leq 1$. In the present work, the capture coefficient has been varied, namely ξ = 0.1, 0.3, 0.6 and 1.0. If the particle is not finally exhausted at the pumping slot, then it undergoes a diffuse reflection, assuming that the temperature at the entrance to the pumping port is equal to 420 K. The total area of the pumping slot is equal to 2.1 m². The surfaces A and B in the HFS and LFS correspond to the virtual windows, through which neutrals penetrate the PFR and on which the incoming boundary conditions are imposed. The corresponding area for each surface is 1.6 m² and 2.8 m² respectively. The surfaces E and F represent the boundaries through which the neutrals

will enter the scrape-off layer (SOL) and it is assumed that they will be immediately ionized and removed from the computational domain. Finally, the height of the dome is constrained by the predefined x-point and in this work the distance of the bottom dome surface from the pumping slot is equal to 1.46 m.

3. Numerical method and boundary conditions

The DIVGAS code, which is based on the Direct Simulation Monte Carlo (DSMC) method [6], has been applied for the numerical modelling of the configuration under consideration. A detailed description of this method is omitted and the reader may consult the following publications [7–10] for further details. Here, only crucial simulation parameters are mentioned. In brief, in all the present simulations an optimum value of time step $\Delta t = 0.01$ μs has been applied. On the other hand, the average number of particles in each simulation ranges between 10^7 and 2×10^7. This number assures that the statistical scattering of macroscopic quantities along the computational domain is sufficiently low. An unstructured tetrahedral grid is applied, with the number of cells to be equal to 2×10^6. The applied grid was chosen such that the cell size is much smaller than the local mean free path. Due to the high collisionality flow regime met in the divertor area, the computational effort is quite challenging. This work was performed on the MARCONI HPC with 200 CPUs for each run, and the typical time for reaching steady state conditions (i.e. the fluctuation of all macroscopic parameters to be less than 1%) was several weeks. For all simulated cases the particle balance of the total incoming and outgoing particles in the flow domain is fully satisfied.

The imposed boundary conditions assume that pure molecular deuterium (D₂) gas enters the sub-divertor area through the virtual windows A and B (see Fig. 2b) with reference pressure P_0 and temperature T_0 equal to 1 and 10 Pa and 4023 K (or 0.35 eV) respectively. The high pressure case consists of a generic assumption based on former ITER relevant detached plasma scenarios as described in [11]. The aforementioned macroscopic quantities P_0 and T_0 define the incoming neutral flux Φ^+, as shown in Fig. 2b, while all the other particle fluxes would be estimated as an outcome of each simulation. The particle flux Φ^+ is yielded by assuming Maxwellian distribution of incoming neutrals using the expression

$$\Phi^+ = \frac{1}{4} S \frac{P_0}{k_B T_0} v_{th}, \tag{1}$$

where S is the area of the virtual windows A and B, k_B the Boltzmann constant and v_{th} is the mean thermal velocity. In addition, the net inlet particle flux $\Phi_{in,net}$ is introduced and is equal to $\Phi_{in,net} = \Phi^+ - \Phi^-$. The pumping efficiency is convenient to be defined as the ratio of Φ_{pump} /$\Phi_{in,net}$ [4], which equals to unity if there are only losses through the pumping slot. Otherwise, this ratio becomes smaller than unity. Therefore, in the following section, all the presented particle fluxes are normalized based on the $\Phi_{in,net}$. Moreover, in the present work the ionization, dissociation and recombination processes on the walls and in the gas phase have not been taken into account. Therefore, when a
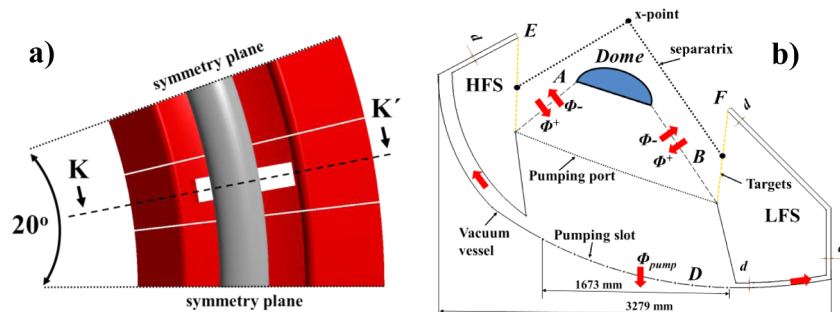
Fig. 2. a) A 20° degree DEMO divertor sector including the dome structure, the plane KK´ as well as the symmetry planes, b) A 2D cut along the KK´ plane.
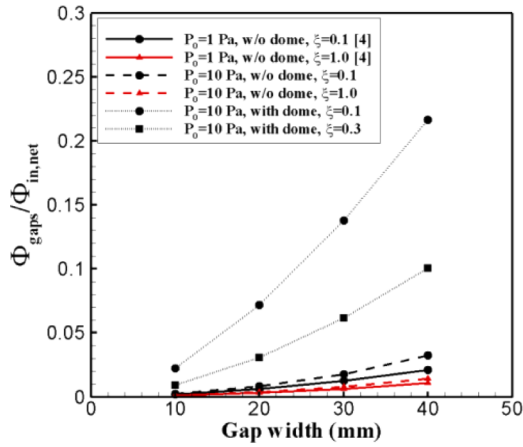
Fig. 3. Normalized particle flux through the toroidal and poloidal gaps in terms of the gap width. The cases with and without dome as well as different incoming boundary conditions and capture coefficients are considered.

Fig. 4. Normalized outflux in terms of the gap width. The case without dome as well as different incoming boundary conditions and capture coefficients are considered.

deuterium molecule hits a stationary wall or the bottom part of the dome, it remains as molecule and a purely diffuse reflection takes place, where the incident molecule is reemitted with Maxwellian distribution based on the wall temperature, equal to $T_{wall} = 420$ K.

4. Results and discussion

4.1. Particle flux through the inter-cassette gaps

In Fig. 3 the normalized particle flux through all the toroidal and poloidal gaps in terms of the gap width is presented, for the cases with and without dome as well as different imposed incoming to PFR boundary conditions and capture coefficients. It is seen that in general the normalized particle flux increases with the gap width, while inverse behavior is observed in the case of the capture coefficient ξ, namely the particle flux through the gaps decreases with increasing capture coefficient. Moreover, the impact of the dome can be seen in Fig. 3. In the case without the dome, the normalized particle fluxes are significantly smaller, and the pressure P_0 of incoming to PFR neutrals, has only a weak impact on the particle flux through the gaps compared with the corresponding case with the dome. The existence of the dome facilitates higher particle fluxes through the gaps and as representative example the reference case of 20 mm gap width is chosen for demonstration purposes. For a capture coefficient equal to ξ = 0.1 and P_0 = 10 Pa, the normalized flux through the gaps is increased by a factor of ∼7 in the case with dome, compared with the corresponding case without one.

4.2. Outflux of neutrals towards the x-point

As it was observed in our recent work [4], in the case without the dome a strong outflux of neutrals moving towards the x-point is observed. The outflux represents almost 80–90% of the incoming neutral particles and is almost independent from the gap width. In Fig. 4, the results of the normalized outflux in terms of the gap width are presented for different capture coefficients ξ and different imposed incoming to PFR boundary conditions. For comparison purposes the results presented in [4] are additionally considered. It is seen that indeed the outflux is weakly dependent on gap width for any capture coefficient ξ and P_0, T_0. On the other hand, when the imposed neutral pressure P_0 increases by an order of magnitude, then the outflux is reduced by about 5%. In general, it is noted that the outflux in the case without dome dominates the gap losses and therefore the effect of the gaps is less pronounced compared with the case with dome.
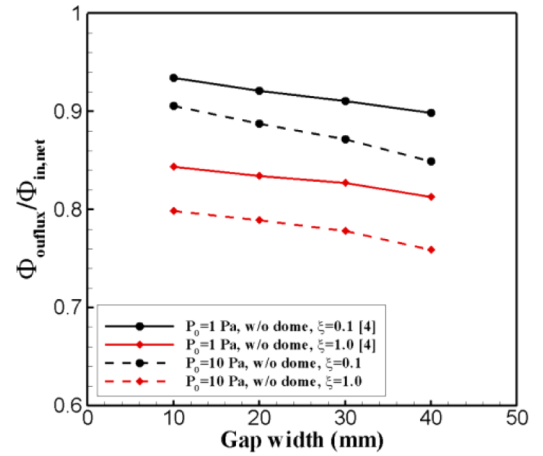
4.3. Pumped particle flux

In Fig. 5a, the normalized pumped flux in terms of the gap width is presented, for the cases with and without dome as well as for different imposed incoming to PFR boundary conditions and capture coefficients ξ. It is observed that in the case without dome, the pumping efficiency is very low and almost independent from the gap width. Moreover, a modest dependence of the pumping efficiency on the incoming boundary conditions is found. The main reason for this behavior is that in both cases, a strong outflux towards the x-point dominates the particle balance in the PFR and results in a very low pumped flux. More specific, for capture coefficient ξ = 0.1 and the reference case of 20 mm gap width, the normalized pumped flux increases by a factor of ∼1.37, as the pressure of the incoming neutrals increases by one order of magnitude. On the other hand, for the case with the dome, the normalized pumped flux (i.e. the divertor pumping efficiency) decreases with increasing gap width, due to the particles losses through the gaps. Furthermore, for the reference case of 20 mm and capture coefficient ξ = 0.1, the pumping efficiency considerably increases by a factor of ∼9 compared with the corresponding case without the dome.

In Fig. 5b, the effective pumping speed S_{eff} of the configuration under consideration in terms of the gap width and two values of ξ is presented. The solid lines correspond to the S_{eff} in the case with dome, defined as $S_{eff} = \Phi_{pump}/P_0$, where Φ_{pump} is the pumped flux through the pumping slot (see Fig. 2b) in Pa m³/s. The dashed lines correspond to the effective pumping speed for the case without dome. For both cases, it is seen that there is a weak dependence of S_{eff} on the gap width for any ξ. On the contrary, a strong dependence of S_{eff} on ξ is observed for any gap width. For the reference case of 20 mm gap width, with the dome structure and ξ = 0.1, the deduced effective pumping speed of the complete divertor ring (i.e. 54 cassettes with 18 pumping slots in total) equals to 44.3 m³/s, while in the case without the dome S_{eff} equals to 32.3 m³/s, namely a factor of ∼1.4 variation.

4.4. 2D vs 3D divertor representation

In order to assess the importance of the present 3D divertor simulations, a comparison is being performed between corresponding (i.e. means subject to the same incoming boundary conditions) 2D and 3D DEMO divertor representations. The considered 2D flow domain corresponds to the 2D cut along the plane KK' (see Fig. 2a and b). The pressure and temperature of the incoming neutral particles were considered equal to P_0 = 10 Pa and T_0 = 0.35 eV respectively. In Table 1, the comparison between corresponding 2D and 3D simulations is being presented. For the reference case of 20 mm gap width and ξ = 0.1, the
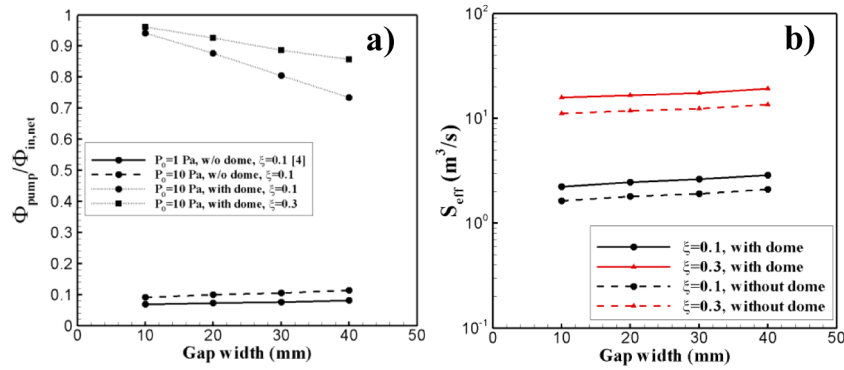
Fig. 5. a) Normalized pumped flux in terms of the gap width. The cases with and without dome as well as different incoming boundary conditions and capture coefficients are considered. b) Effective pumping speed in terms of the gap width for the case with and without the dome and for various capture coefficients.

Table 1
Normalized pumped flux $\Phi_{pump}/\Phi_{in,net}$ considering a 2D and 3D divertor representation.

	2D	3D	Δ (%)	2D	3D	Δ (%)
Gap width (mm)	ξ = 0.1	ξ = 0.1		ξ = 0.3	ξ = 0.3	
20	0.877	0.981	10.6	0.926	0.993	6.7
40	0.735	0.937	21.5	0.857	0.977	12.3

relative difference between 2D and 3D representations is 10.6% and increases further as the gap width is increased. The same behavior is being observed for the case of the higher capture coefficient ξ = 0.3. In general, it is deduced that as the gap width increases, the need to perform more detailed and time-consuming simulations, becomes of great importance.

5. Conclusions

In the present work a parametric analysis by using the DIVGAS code is performed in order to highlight the influence of the inter-cassette gaps and the existence of the dome on the pumping efficiency of the DEMO divertor. For this fundamental study, a 3D divertor configuration is chosen, in which D_2 neutral particles are assumed to penetrate the PFR. The chosen incoming boundary conditions correspond to a high-collisionality divertor case. According to our previous work the separatrix losses dominates any losses due to the gap leakages under the assumptions of no dome and lower divertor pressure levels. In the present work, a more generic model based on the existence of dome and higher divertor pressure expected in DEMO has been considered.

Based on the presented results, it can be concluded that in the case without the dome the particle losses through the separatrix are dominating and consequently the effect of 3D leakages on the pumping efficiency is small. To avoid these particle losses, for the reference case of 20 mm gap width and low capture coefficients, the addition of the dome increases the pumping efficiency 9 times compared to the case without the dome. The dome eliminates the outflux of neutrals towards the x-point and forces the neutrals to move downwards in the sub-divertor vicinity. Therefore, a neutral compression is being achieved, which facilitates the increase of the pumping efficiency. In general, it is concluded that the dome provides a first order variation in pumping efficiency in comparison to the case of the divertor without the dome, while the gap leakages provide a second order variation, which seems to be more important when the dome is present.

With regard to DEMO, it has to be noted that the divertor design will

have to reconcile also other requirements than those for particle exhaust as discussed in this paper. It is obvious that the gaps between the divertor cassettes cannot be completely eliminated due to manufacturability and accessibility in this area. The final design will hence be decided when the trade-offs between various options can be better evaluated.

Supplementary materials

Supplementary material associated with this article can be found, in the online version, at doi:10.1016/j.nme.2019.02.021.

References

[1] D.P. Stotler, B. LaBombard, Three-dimensional simulation of gas conductance measurement experiments on Alcator C-Mod, J. Nucl. Mater. 337–399 (2005) 510–514.
[2] A.S. Kukushkin, H.D. Pacher, V. Kotov, D. Reiter, D. Coster, G.W. Pacher, Effect of conditions for gas recirculation on divertor operation in ITER, Nucl. Fusion 47 (7) (2007) 698–705.
[3] V. Hauer, Chr. Day, ITER divertor gas flow modelling, FED 98-99 (2015) 1775–1778.
[4] S. Varoutis, et al., Effect of neutral leaks on pumping efficiency in 3D DEMO divertor configuration, FED 136 (2018) 1135–1139, https://doi.org/10.1016/j.fusengdes.2018.04.089.
[5] R. Wenninger, et al., The physics and technology basis entering European system code studies for DEMO, Nucl. Fusion 57 (2017) 016011.
[6] G.A. Bird, Molecular Gas Dynamics and the Direct Simulation of Gas Flows, Oxford University Press, Oxford, UK, 1994.
[7] S. Varoutis, et al., Simulation of neutral gas flow in the JET sub-divertor, FED 121 (2017) 13–21.
[8] S. Varoutis, et al., Optimization of pumping efficiency and divertor operation in DEMO, Nucl. Mater. Energy 12 (2017) 668–673.
[9] F. Bonelli, et al., Self-consistent coupling of DSMC method and SOLPS code for modeling tokamak particle exhaust, Nucl. Fusion 57 (6) (2017) 066037.
[10] Chr. Day, S. Varoutis, Yu. Igitkhanov, Effect of the dome on the collisional neutral gas flow in the DEMO divertor, IEEE Trans. Plasma Sci. 44 (9) (2016) 1636–1641.
[11] A.S. Kukushkin, H.D. Pacher, V. Kotov, D. Reiter, D. Coster, G.W. Pacher, "Effects of the dome on divertor performance in ITER", J. Nucl. Mater. 363–365 (2007) 308–313.